Tests of One-Way Post-Tensioned Slabs With Unbonded Tendons

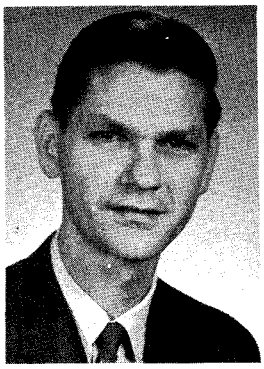

Ned H. Burns
Professor of Civil Engineering
The University of Texas at Austin
Austin, Texas

Finley A. Charney*
Associate
Walter P. Moore & Associates, Inc.
Houston, Texas

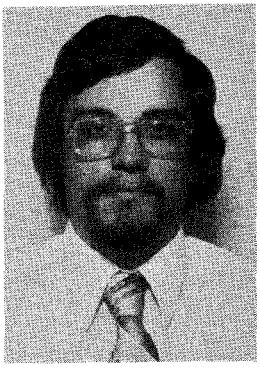

Wendell R. Vines*
Project Engineer
TERA, Inc.
Houston, Texas

The provisions in the ACI Building Code (ACI 318-77)[1] for prestressed concrete recognize a difference in the amount of mild steel required for ultimate strength and crack control between bonded and unbonded members. However, the ACI Code equations are based mainly on experience with and tests on beams with relatively low span/depth ratios compared to those common with post-tensioned slabs.

Previous research efforts concerning members with unbonded tendons and various span/depth ratios have shown that the ACI Code expressions for steel stress at ultimate may be unconservative for members such as slabs with span/depth ratios as high as 40 or more,[2,3] while reinforcement required for crack control may be on the conservative side.

*Formerly Research Assistants, The University of Texas at Austin.

Synopsis

Tests of two half-scale slabs with unbonded tendons for post-tensioning and differing amounts of bonded reinforcement were carried out at The University of Texas at Austin.

Both slabs had three equal spans with a span/depth ratio of 44. One slab had $6\sqrt{f_c'}$ ($0.50\sqrt{f_c'}$) tension at service load and the bonded reinforcement for strength was less than the current ACI Code requirement.

The other slab had $9\sqrt{f_c'}$ ($0.75\sqrt{f_c'}$) tension at service load and the bonded reinforcement was slightly more than the required minimum requirement.

Satisfactory distribution of cracking and strength were obtained for both slabs. Also, satisfactory overall performance was shown to be provided by the slab having $9\sqrt{f_c'}$ ($0.75\sqrt{f_c'}$) tension at service load.

Deflection calculations based on an effective moment of inertia give realistic though slightly conservative results as compared to the deflections measured in the tests.

Computed ultimate loads compared favorably with those measured for both slabs, and the strength met the ACI Code requirements.

In order to obtain a better understanding of partially prestressed concrete slabs with unbonded tendons, a test program was carried out at The University of Texas at Austin during which the strength and behavior of two half-scale models of prototype structures were experimentally evaluated.[4,5] Of major concern was the comparison of observed behavior with that predicted following the provisions of ACI 318-77.

The specific objectives of the test program were to:

1. Examine the load-deflection response of the slabs before and after initial cracking with particular attention to the effects of cracking on the observed stiffness of the two slabs.
2. Observe the control and distribution of cracking provided by different amounts of bonded non-prestressed reinforcement.
3. Determine experimentally the ultimate strength of the specimens as well as measure the increase in tendon stresses as failure loads were approached.
4. Compare the test results with the provisions contained in ACI 318-77.

Selection of Test Specimens

Prestressed concrete elements are normally proportioned on the basis of some limiting stress in the concrete at service load, and then checked for ultimate strength. Depending on the magnitude of the tensile stress in the concrete, the service load deflections may or may not be elastic.

Under normal circumstances, the limiting tensile stress is $6\sqrt{f_c'}$ ($0.50\sqrt{f_c'}$) and the concrete remains uncracked throughout the service load range. Section 18.4.2 of the ACI Code, however, allows tensile stresses as

Table 1. Design parameters of prototype structures for Slabs A and B.

Parameter	Prototype for Slab A	Prototype for Slab B
Span	20 ft.	20 ft.
Slab thickness	5.5 in.	5.5 in.
Design live load	50 psf	50 psf
Allowable tension in concrete at service load	$6\sqrt{f_c'}$	$9\sqrt{f_c'}$
f_c'	4000 psi	4000 psi
f_{pu}	240 ksi	240 ksi
f_{py}	213 ksi	213 ksi
P/A stress	185 psi	140 psi
Initial tendon stress	140 ksi	140 ksi
Percent unbonded reinforcement	0.120	0.098
Percent bonded reinforcement	$0.12 < 0.20$ required by ACI Code	$0.23 > 0.20$ required by ACI Code

*Two adjacent spans loaded with live load and dead load on all spans.
Note: 1 psi = 6.9 kN/m²; 1 ksi = 6.89 MPa; 1 ft = 0.305m; 1 in. = 25.4 mm; 1 lb = 4.45 N.

high as $12\sqrt{f_c'}$ ($1.00\sqrt{f_c'}$), so long as careful deflection computations are made to insure satisfactory performance. With service load stresses of $12\sqrt{f_c'}$ ($1.00\sqrt{f_c'}$) the concrete would certainly be cracked ($f_r = 7.5\sqrt{f_c'}$ or $0.62\sqrt{f_c'}$) and inelastic action would be evident in the working load range.

In addition to the requirements for maximum tensile stresses in the concrete, ACI 318-77 states a minimum requirement for bonded reinforcement when unbonded tendons are used:

$$A_s = 0.004A \qquad \text{[ACI Eq. (18-5)]}$$

where

A_s = minimum bonded steel, sq in.
A = area of that part of the cross section between the flexural tension face and the center of gravity of cross section, sq in.

Eq. (18-5) requires that A_s for a solid slab equal to 0.2 percent of the cross-sectional area be supplied as bonded reinforcement, and a primary question to be addressed by these tests is whether this amount of A_s is realistic as a minimum requirement.

Two slabs were experimentally evaluated incorporating characteristics to test the adequacy of the ACI Code design requirements. The main variables in the two specimens were the allowable tensile stress in the concrete at service load and the amount of bonded reinforcement. In Slab A, the tensile stresses were limited to $6\sqrt{f_c'}$ ($0.50\sqrt{f_c'}$) and in Slab B, the design tensile stresses under service load were $9\sqrt{f_c'}$ ($0.75\sqrt{f_c'}$). In both cases the bonded reinforcement provided was that required for strength, even if that amount were less than that

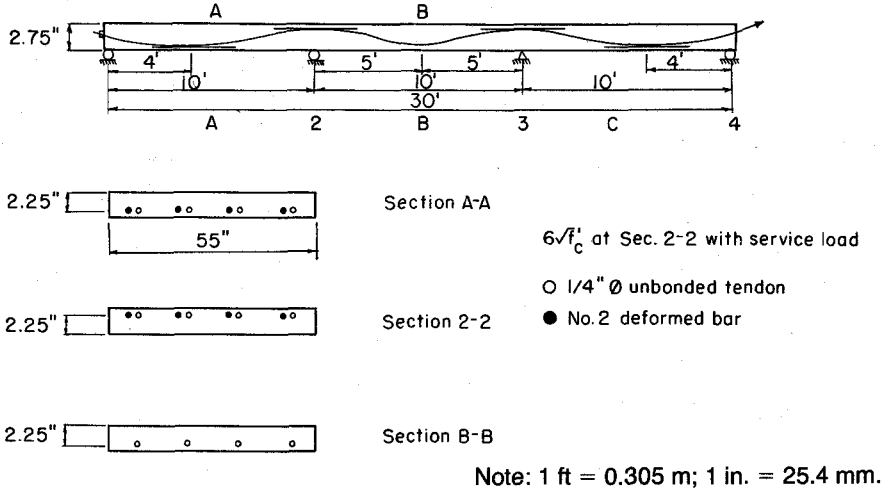

Fig. 1a. Plan and section of Slab A (ideal model).

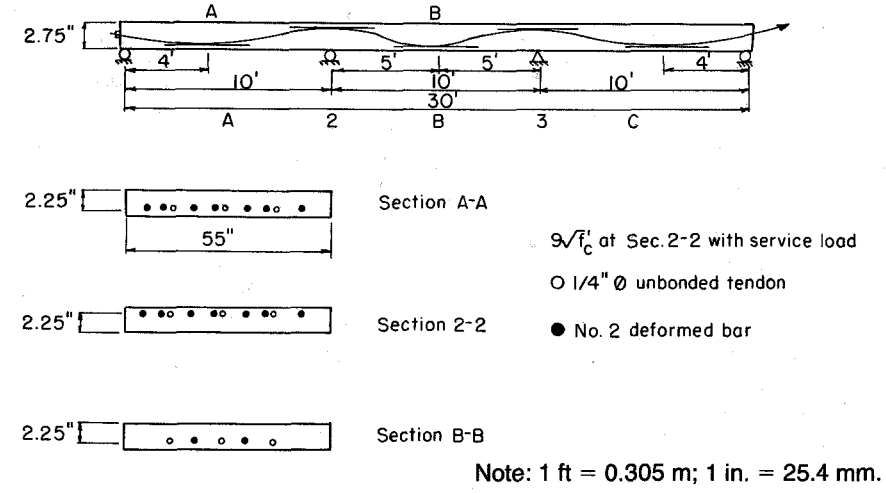

Fig. 1b. Plan and section of Slab B (ideal model).

specified under Section 18.9 of the ACI Code. For Slab A (prototype and model) the bonded reinforcement was 0.12 percent of cross-sectional area which is less than the 0.20 percent required by the ACI Code.

The physical dimensions of the prototype slabs were the same for both specimens; three equal spans of 20 ft (6 m) each, and a thickness of 5.5 in. (140 mm).

Table 1 lists the design parameters for the prototype structures. Test slabs A and B were half-scale models from these designs.

Figs. 1a and 1b show a plan and section views for the two slab specimens.

Materials and Fabrication

With the design conditions known, the two one-half scale model structures (Slab A and Slab B) were proportioned accordingly. By matching the *P/A* stresses in the prototype, the width of the specimens was set as 55 in. (1400 mm). Using this width, scaling all other dimensions down to one-half, and replacing the weight of concrete lost due to scaling, the models would be stressed exactly as would the prototype under similar loading conditions.

The prototype slabs and half-scale models were designed for a 28-day compressive concrete strength of 4000 psi (27.58 MPa). The observed strength for the models was higher with a measured average cylinder strength of 4700 psi (32.41 MPa) for Slab A and 5150 psi (35.51 MPa) for Slab B. The unbonded tendons were ¼ in. (6.3 mm) diameter single wire with a measured ultimate strength of 240 ksi (1655 MPa). The tendons were coated with mastic and wrapped in reinforced waterproof paper to prevent bond to the concrete. The bonded reinforcement was deformed bar of 6 mm diameter (#2 bar) with a yield stress of 65 ksi (448 MPa).

The specimens were cast in place over pedestals which provided line support across the width of the slab. Refer to Fig. 2 for the nomenclature used in this paper for identifying supports and spans.

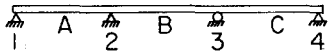

Fig. 2. Identifying nomenclature.

Instrumentation

Both slabs were extensively instrumented. Stresses in tendons and bonded reinforcement were monitored using strain gages. Midspan and quarter span deflections were measured electronically and checked manually with dial gages. Load cells monitored interior support reactions, applied loads, and force in the unbonded tendons.

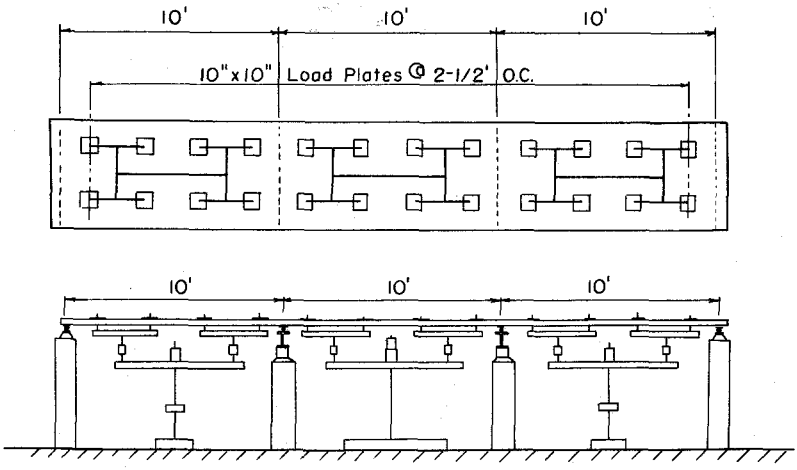

Fig. 3. Plan and elevation of loading system used in tests.
Note: 1 ft = 0.305 m; 1 in. = 25.4 mm.

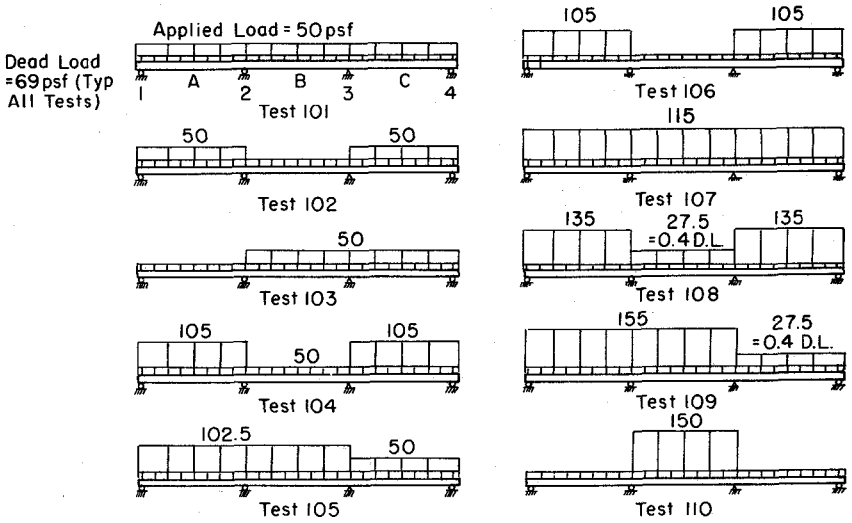

Fig. 4a. Load patterns for Slab A. Note: 1 psf = 47.9 Pa.

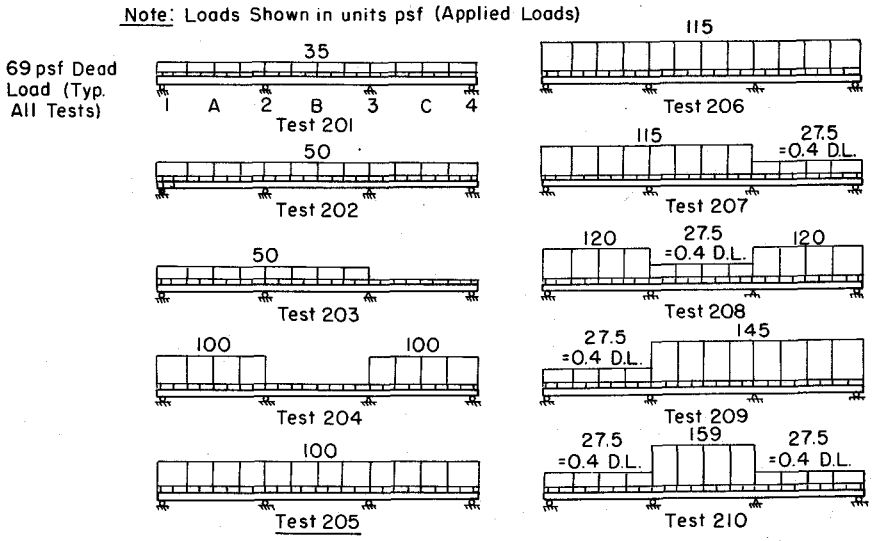

Fig. 4b. Load patterns for Slab B. Note: 1 psf = 47.9 Pa.

Test Procedure

Pattern loadings designed to produce maximum stress at each critical section were imposed on the slabs. Fig. 3 illustrates the whiffle tree mechanism used to simulate a uniform load on the slabs. The specimens were tested through three load ranges: elastic, inelastic (cracked), and ultimate.

Figs. 4a and 4b show the patterns of loadings used in the tests. Load levels

shown in these figures as well as in other figures in this discussion refer to *applied loads* only, and as such do not include slab dead weight or dead weight replacement. The elastic phase of testing (first four tests) served to calibrate the slab and to produce cracking for later tests.

The inelastic behavior was investigated during the next three tests to determine the effects of cracking on reduced stiffness, and to measure the response of the initially cracked specimen under various patterns of load. After each slab was thoroughly cracked, it was then loaded in three final test patterns until a failure had occurred in each span. In these particular tests, the ultimate flexural capacity and the increases in unbonded tendon stress were measured.

Test Results

The test results are given first for Slab A and then for Slab B.

Slab A

Tests 101 to 104 tested the elastic behavior of Slab A, with Test 104 producing first cracking. This slab was designed for tensile stresses of $6\sqrt{f'_c}$ $(0.50\sqrt{f'_c})$ at working loads. Fig. 5 shows the load-deflection curves for these tests, indicating linear elastic behavior associated with uncracked section properties.

In all cases the load-deflection response of the slab coincided with the predicted behavior as calculated on the basis of gross cross section. Test 104 [in which the exterior spans were loaded in 5-psf (240 Pa) increments to 105 psf (5030 Pa), and the interior span was loaded to 50 psf (2395 Pa)], produced first cracking at a load level of 102.5 psf (4910 Pa), when a hairline crack was detected on the top surface of the slab over Support 3.

Tests 105 to 107 loaded an initially cracked specimen, with damage due to cracking increasing as loading proceeded. The slopes of the load-deflection curves indicated a reduced stiffness as compared to the uncracked predictions of deflection as shown by the dashed lines in Fig. 6. The extent of flexural cracking through Test 107 consisted of hairline cracks at support sections 2 and 3 (top of slab) with single hairline cracks approximately $0.4L$ from the end supports (bottom of slab). This indicates minor damage even for levels of load reaching factored design loads.

Fig. 7 shows the load-deflection behavior during Tests 108, 109, and 110 which produced failures in Spans C, A, and B, respectively. For tests 108 and 109 failure was preceeded by the formation of numerous flexural cracks in the positive moment regions of the loaded spans as shown in Fig. 8. The location of the positive moment failure cracks was at 4 ft (1.2 m) from the interior supports, which coincided with the cutoff point of the positive moment bonded reinforcement.

As shown in Fig. 7, the load-deflection response of the slab indicates failure at about the time these large cracks formed. Note that failure was defined as increased deflection with no increase in load, since a compression failure of the concrete did not occur. For Test 110, where the middle span was loaded until a failure occurred, the maximum applied load reached 150 psf (7185 Pa). Although no bonded reinforcement was provided, this failure was also forewarned by the formation of a large flexural crack. Collapse was confirmed by the crushing of concrete in Span B. The extent of flexural cracking in Slab A through Test 110 is shown in Fig. 8.

Besides determining the ultimate strength of Slab A, the increases in unbonded tendon stresses were measured by strain gages bonded to the tendons. As shown in Fig. 9, the in-

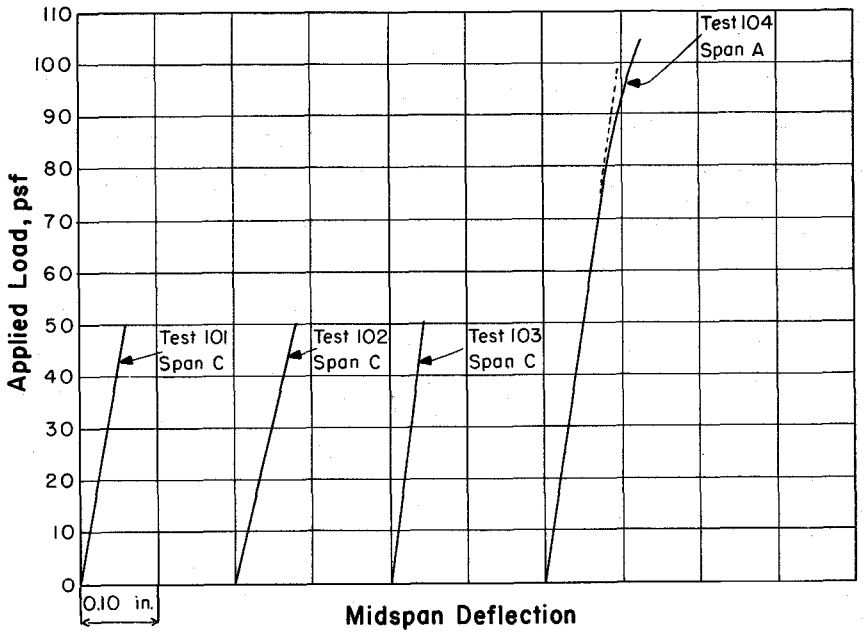

Fig. 5. Load vs. deflection curves for Tests 101-104.
Note: 1 psf = 47.9 Pa; 1 in. = 25.4 mm

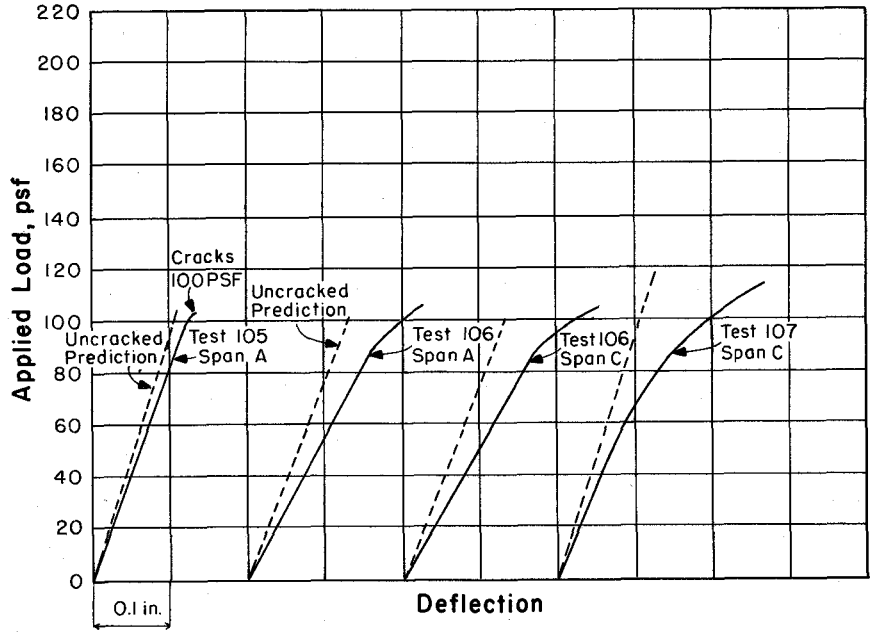

Fig. 6. Load vs. deflection for Tests 105-107.
Note: 1 psf = 47.9 Pa; 1 in. = 25.4 mm.

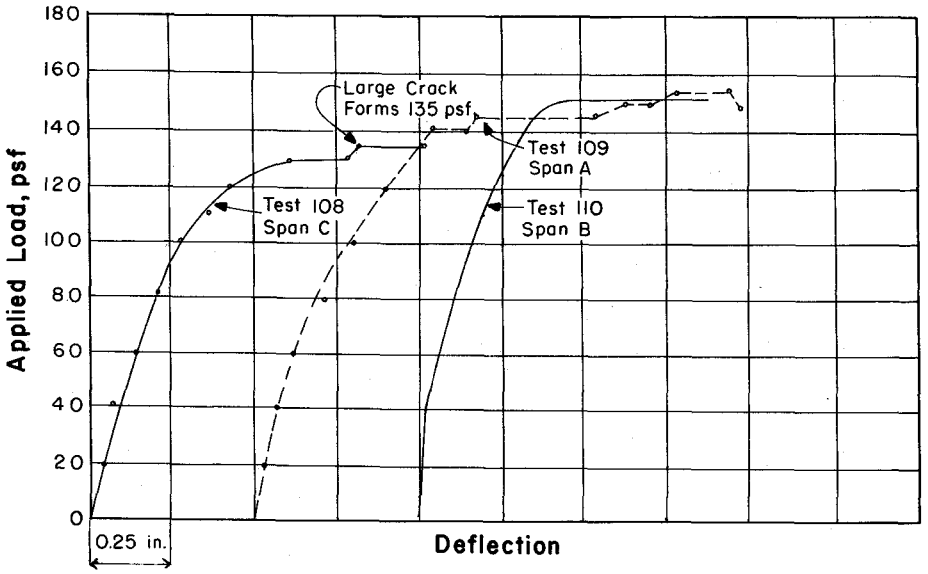

Fig. 7 Load vs. deflection for Tests 108-110. Note: 1 psf = 47.9 Pa; 1 in. = 25.4 mm.

creases in unbonded tendon stresses for Tests 108 to 110 were relatively low until the failure cracks had formed and large deflections occurred, at which point the tendon stresses rapidly increased. The maximum measured tendon stress increase was 19.5 ksi (134.45 MPa) which occurred during Test 109.

Slab B

Slab B was also subjected to ten separate load tests, as shown in Fig. 4b. With the design tensile stress of $9\sqrt{f_c'}$ ($0.75\sqrt{f_c'}$) load, the specimen would be cracked at that stress level for any load pattern.

Test 201 to 204 measured the elastic response of the specimen to applied load. As shown in Fig. 10, the load-deflection curve indicated linear elastic behavior up to the load level of 50 psf (2395 Pa), but in Test 204, where the maximum load reached 100 psf (4790 Pa), visible cracking occurred in Span C only after the final load in-

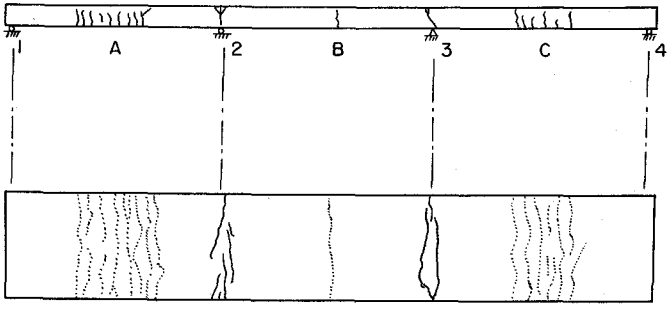

Fig. 8. Crack pattern through Test 110 for Slab A.

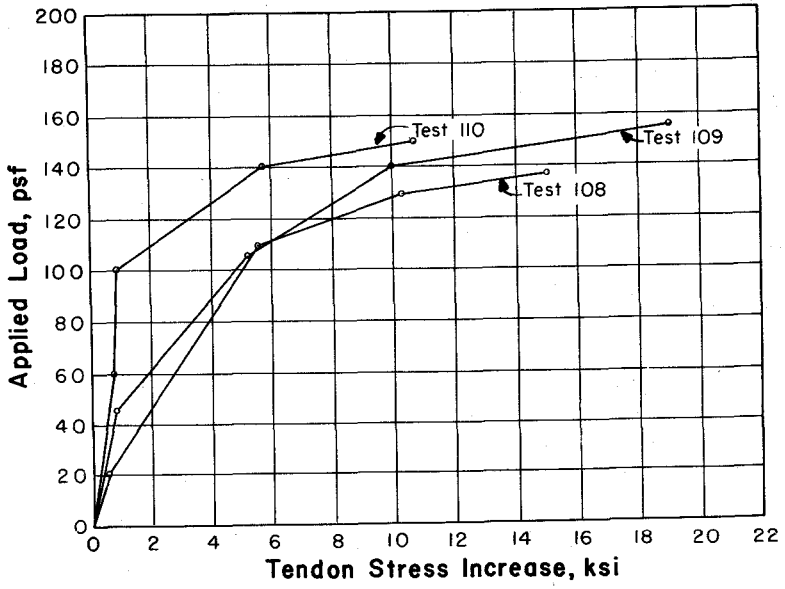

Fig. 9. Tendon stress increase vs. applied load for Tests 108-110.
Note: 1 psf = 47.9 Pa; 1 ksi = 6.89 MPa.

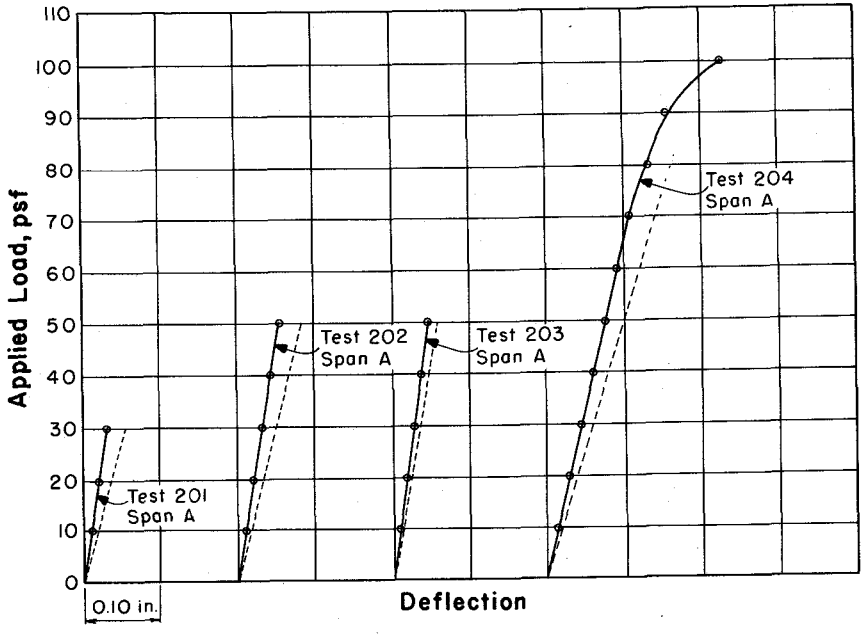

Fig. 10. Load vs. deflection for Tests 201-204.
Note: 1 psf = 47.9 Pa; 1 in. = 25.4 mm.

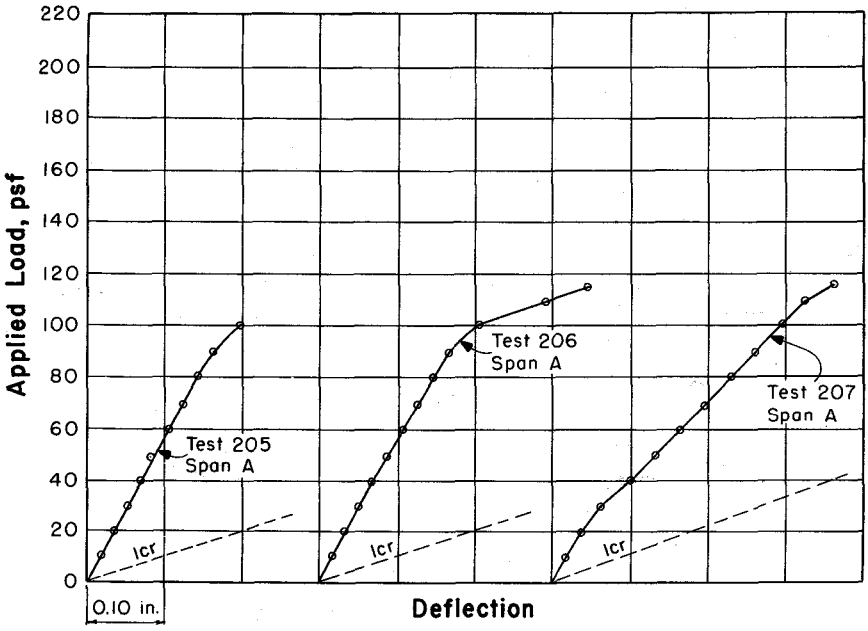

Fig. 11. Load vs. deflection for Tests 205-207. Note 1 psf = 47.9 Pa; 1 in. = 25.4 mm.

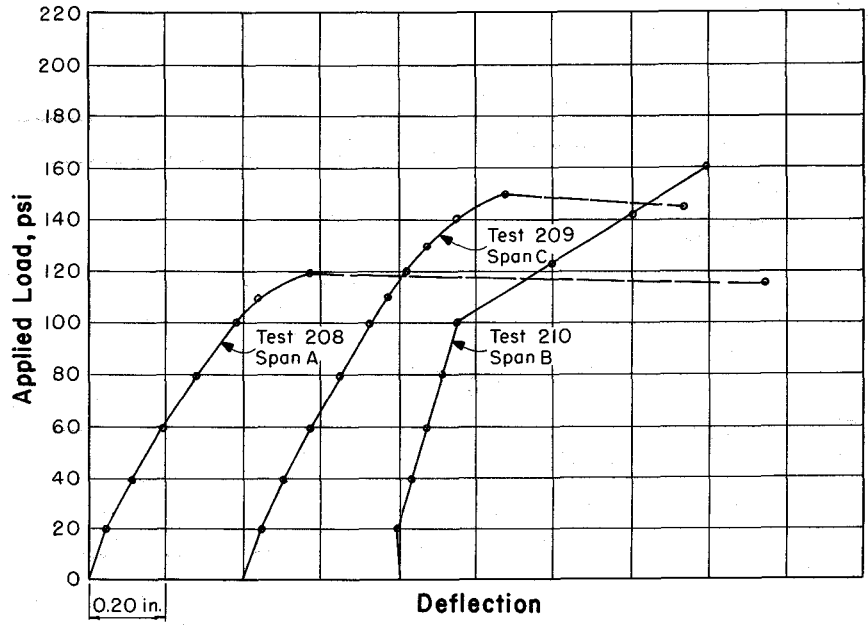

Fig. 12. Load vs. deflection for Tests 208-210. Note: 1 psf = 47.9 Pa; 1 in. = 25.4 mm.

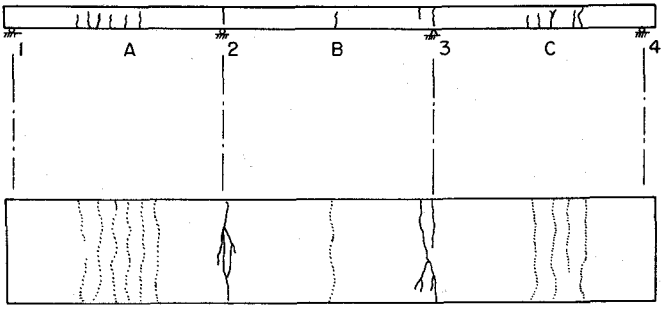

Fig. 13. Crack patterns after Test 210.

crement was added. The predicted elastic response for Slab B, as shown by the dashed lines in the curves of Fig. 10, possesses a lower stiffness than observed during testing.

Tests 205 to 207 loaded an initially cracked specimen, with damage due to cracking increasing as load proceeded. In each case, the specimen possessed an inelastic stiffness lower than elastic yet not as low as predicted by a transformed cracked section moment of inertia as shown in Fig. 11. The extent of flexural cracking through Test 207 was minor, with the hairline cracks at Supports 2 and 3 (top cracks) and at approximately $0.4L$ from support (single bottom cracks) in the end spans.

Failure mechanisms of Tests 208 and 209 were initiated by the formation of large flexural cracks in the positive moment regions where the bonded reinforcement had been cut off. In Test 208, the failure crack formed at 4 ft (1.22 m) from Support 2 at the rebar cutoff point. In Test 209 the large crack formed 2 ft (0.61 m) from the exterior support 4, also near the reinforcing bar cutoff point.

Due to the nonexistence of bonded reinforcement within these failure locations, deflections grew rapidly producing rotations with the deflected shape being rather angular. Note that failure was defined as increasing deflection with no increase in load.

For Test 210, the failure was accompanied by a compression failure at midspan of Slab B. Fig. 12 illustrates the load-deflection curves for Tests 208 through 210, and Fig. 13 shows the crack patterns present on the surface of the slab upon completion of testing Slab B.

The increases in unbonded tendon stresses in Slab B as measured during Tests 208-210 are shown in Fig. 14. The greatest tendon stress increase was measured in Span A during Test 208, with a magnitude of 21 ksi (145 MPa).

Discussion of Results

In the working load range, both Slab A and Slab B behaved well, with deflection and cracking serviceability remaining under good control. It was observed that the immediate service load deflections measured were well within the limits as set up by Chapter 9 of the ACI Code. Table 2 lists the observed deflections measured in terms of the span length. All of the service load deflections fall well below $l/360$.

In the case of Tests 105 to 108, and 205 to 208, the specimens were initially cracked and possessed a flexural stiffness less than that of the elastic gross section. For Slab A, where the limiting tensile stress was $6\sqrt{f_c'}$

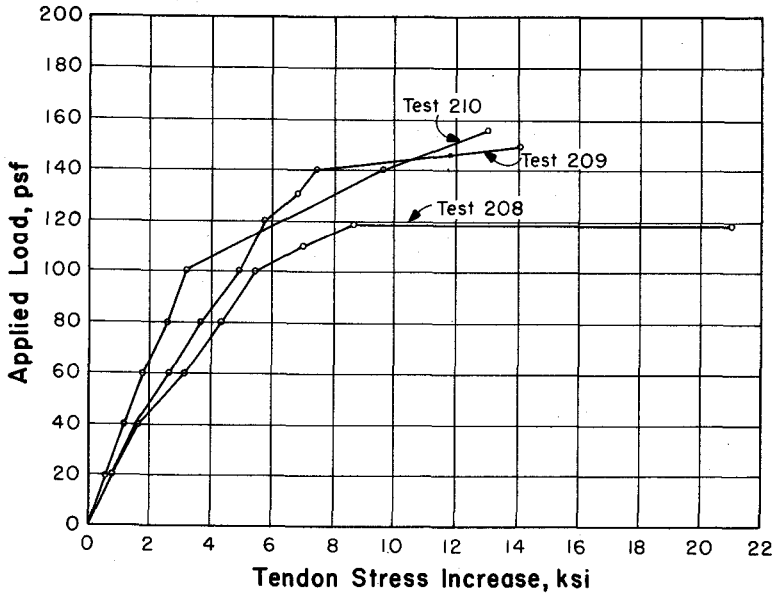

Fig. 14. Applied load vs. tendon stress increase for Tests 208-210.
Note: 1 psf = 47.9 Pa; 1 ksi = 6.89 MPa.

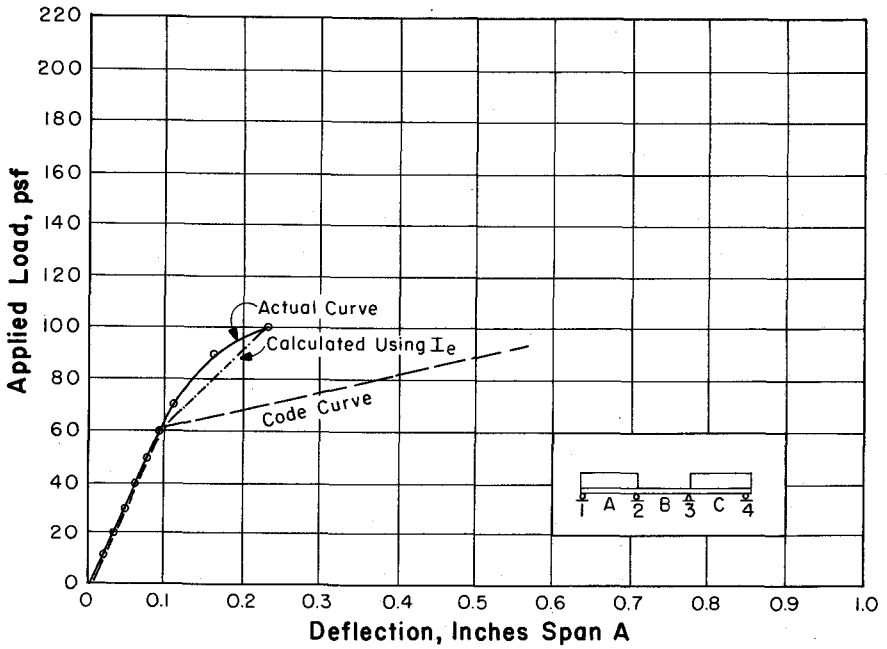

Fig. 15. Load vs. deflection for Test 204. Note: 1 psf = 47.9 Pa; 1 in. = 25.4 mm.

Table 2. Deflections at service load.*

Slab ID	Test No.	Spans loaded	in.	Span / Constant
Slab A	104	A,C†	0.059	//2033
	105	A,B	0.053	//2264
	106	A,C	0.087	//1379
	107	A,B,C	0.065	//1846
	108	A,C†	0.105	//1142
Slab B	204	A,C	0.100	//1200
	205	A,B,C	0.112	//1071
	206	A,B,C	0.118	//1017
	207	A,B	0.177	//678
	208	A,C	0.211	//569

*Deflections are shown for a service live load of 50 psf for Slab A, 62.7 psf for Slab B.
†Span B was slightly loaded.
Note: 1 in. = 25.4 mm; 1 psf = 47.9 Pa).

($0.50\sqrt{f'_c}$) no cracking was recorded at design service load, and deflections followed elastic behavior since the full cross section was effective in contributing to elastic stiffness. For Slab B, where the specimen was cracked at service load due to the relatively high tensile stress of $9\sqrt{f'_c}$ ($0.75\sqrt{f'_c}$) in the precompressed tension zone, the actual cracks were few with only a very narrow width. As shown in Test 204, the deflection response to applied load remained relatively elastic through the service load range, although cracks were present.

While initially uncracked or only slightly cracked, both specimens behaved in a nearly elastic manner, but the behavior was inelastic for tests where cracking was substantial at the onset of loading. It is quite possible that an actual structure designed for $9\sqrt{f'_c}$ ($0.75\sqrt{f'_c}$) similar to prototype Slab B may be initially cracked, thus altering the predicted elastic or near elastic behavior.

As shown in the test results, the behavior of the initially cracked specimen lies between purely elastic, and completely inelastic limits as based on the transformed cracked section moment of inertia. It is likely, therefore, that deflection computations based on elastic section properties may be unconservative, especially when there is a high probability that the section may be initially cracked.

When the design allowable tensile stress in the precompressed tension zone of a member is between $6\sqrt{f'_c}$ ($0.50\sqrt{f'_c}$) and $12\sqrt{f'_c}$ ($1.00\sqrt{f'_c}$), ACI 318-77 requires that deflections be based on a bilinear moment-curvature relationship, and the transformed cracked section moment of inertia. Fig. 15 shows such a bilinear load-deflection curve as computed for Test 204, Slab B, as compared to the actual measured curve.

Also shown in Fig. 15 is the predicted load-deflection behavior after cracking based on a modified form of ACI Eq. (9-7) for calculating an effective moment of inertia. ACI Eq. (9-7) is given in Section 9.5.2.3 of the ACI Code as a method for computing an effective moment of inertia, I_e, for use in deflection calculations of non-prestressed one-way slabs and beams:

$$I_e = \left(\frac{M_{cr}}{M_a}\right)^3 I_g + \left[1 - \frac{M_{cr}}{M_a}\right]^3 I_{cr}$$

where

Table 3. Measured vs. ACI Code ultimate tendon stress.

Slab ID	Test No.	f_{se} (ksi)	Observed		Calculated		$\frac{f_{ps}\text{ (obs)}}{f_{ps}\text{ (ACI)}}$
			Δf_{ps} (ksi)	f_{ps} (ksi)	Δf_{ps} (ksi)	f_{ps} (ksi)	
Slab A	108	141.5	15.6	157.1	30.3	171.8	0.91
	109	141.5	19.5	161.0	30.3	171.8	0.94
	110	141.5	10.6	152.1	30.3	171.8	0.89
Slab B	208	146	21	167	53.4	199.4	0.84
	209	146	14	160	53.4	199.4	0.80
	210	146	13	159	53.4	199.4	0.79

Note: 1 ksi = 6.89 MPa.

M_{cr} = cracking moment (tensile stress = $7.5\sqrt{f_c'}$ or $0.62\sqrt{f_c'}$)
M_a = maximum moment in which deflection is being computed
I_g = cross section moment of inertia
I_{cr} = transformed cracked section moment of inertia

Although the intended use of Eq. (9-7) is for non-prestressed members, it can be adapted to prestressed concrete by using the following expression for M_{cr}:

$$M_{cr} = \frac{I_g}{c}(7.5\sqrt{f_c'} + f_{pe} - f_d)$$

where
c = depth from centroid to extreme fiber
f_{pe} = stresses due to prestress
f_d = dead load stress
I_g = gross cross section moment of inertia

Using this procedure the load deflection curve labeled I_e of Fig. 15 was calculated. As shown on the figure, the curve computed on the basis of I_e predicts post-cracking deflection better than does the curve based on a transformed cracked section moment of inertia.

In both Slabs A and B, cracking was well distributed by the bonded reinforcement. In Slab A, the bonded steel consisted of four #2 bars in each maximum moment section (Spans A and C and over Supports 2 and 3). This A_s amounts to only 0.12 percent of the cross section as compared to 0.20 percent required by ACI Eq. (18-5).

The provision of 0.12 percent bonded steel in Slab A provided adequate crack control, thus the requirements of Eq. (18-5) would provide very good behavior with more bonded reinforcement (0.2 percent of area). For Slab B, where seven #2 bars (0.23 percent of the cross section) provided bonded reinforcement, the control of cracking was very similar to that of Slab A.

The increase in unbonded tendon stress at ultimate load did not reach the value predicted by Eq. (18-4) of ACI 318-77. This equation is a conservative version of the lower bound empirical formula developed by Mattock *et al*[6] in a research program testing beams with a ratio of span to overall depth of 28.

Table 3 shows the measured versus computed steel stresses for Slabs A and B. The measured values were consistently less than the calculated increase, but this has substantially a

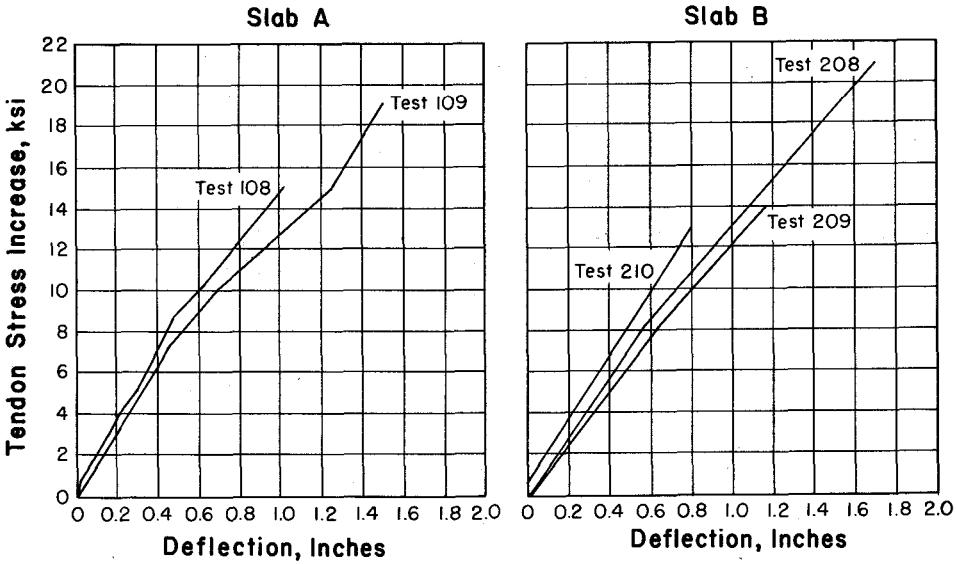

Fig. 16. Tendon stress increase vs. deflection. Note: 1 ksi = 6.89 MPa; 1 in. = 25.4 mm.

smaller effect in ultimate strength calculations since it is the total stress which is considered there. Also, the bonded reinforcement for both specimens supplied a significant portion of the tensile force which is effective in resisting external moments.

Figs. 9 and 14 illustrate how the tendon stresses increased with applied load. These curves have a shape which is very similar to the load-deflection curves for their respective tests (as shown in Figs. 7 and 12). Tendon stress increases plotted against deflections form what is virtually a straight line. Inspection of Fig. 16 indicates that deflections in the order of 4 to 5 m. (102 to 127 mm) would be required for tendon stresses to reach those predicted by the ACI Code equation for these slabs.

Such deflections probably would not have occurred in Slabs A and B without failure even if the reinforcing bars were extended in length according to the requirements of the ACI Code on development length. It would seem then that the ACI equation for stress at ultimate in unbonded tendons, although adequate for lower span to depth ratios, is unconservative for the case where the ratio is as high as 45, as in Slabs A and B. Similar results were discussed in flat plate and slab research by Hemakom.[2,3]

For all tests in which a failure occurred, the ultimate load carried was greater than the factored design load equal to 1.4(69) + 1.7(50) = 182 psf (8718 Pa), and in all cases except Test 208, the loads carried exceeded 182/0.9 = 202 psf (9676 Pa). Due to the type of failures in Tests 108, 109, and 205 and 209, where the positive moment hinge (yield line) formed at or near the reinforcing bar cutoff point the collapse was somewhat premature.

In Test 208 the failure was definitely premature, partly because of the effect of patterned loads on redistribution of moments. Previous hinging over Supports 2 and 3 had an effect on the strength exhibited by Span B of both slabs, resulting in the test load falling below that predicted for Tests 110 and 210.

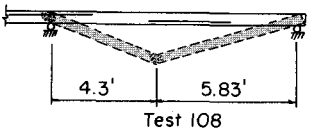

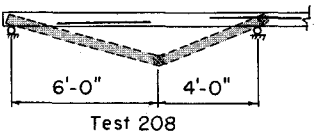

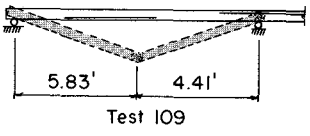

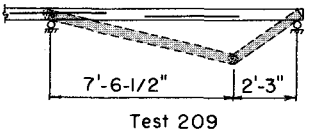

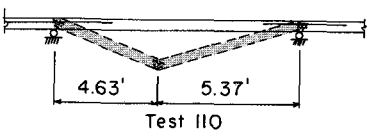

Fig. 17. Failure mechanisms for Tests 108-110. Note: 1 ft = 0.305 m.

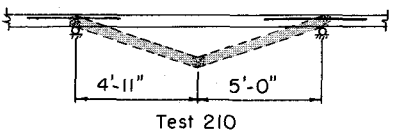

Fig. 18. Failure mechanisms for Tests 208-210. Note: 1 ft = 0.305 m; 1 in. = 25.4 mm.

Table 4 shows the actual load (including dead load) carried for all tests in which a failure occurred. Also shown in the table is the calculated load based on the full ACI Code unbonded tendon stress, the yield in bonded reinforcement, and the positive moment hinge being located at the position in the span which produces the minimum ratio of internal work to external work. Figs. 17 and 18 show the position of the bonded reinforcement within the failure mechanism for each test.

Table 4. Ultimate loads carried by slabs (psf).

Slab ID	Test No.	Spans loaded	Failure span	Ultimate load	Yield line load	Ultimate load / Yield line load
Slab A	108	A,C	C	206	216	0.954
	109	A,B	A	226	222	1.002
	110	B	B	221	278	0.795
Slab B	208	A,C	A	184	170	1.08
	209	B,C	C	214	205	1.04
	210	B	B	228	239	0.954

Note: 1 psf = 47.9 Pa.

Conclusions

From the results of this test program the following conclusions can be drawn:

1. Load-deflection responses measured during testing show that both Slab A and Slab B, designed for $6\sqrt{f'_c}$ $(0.50\sqrt{f'_c})$ or $9\sqrt{f'_c}$ $(0.75\sqrt{f'_c})$, respectively, remained serviceable under working load.

2. The bonded reinforcement which consisted of #2 deformed bars with A_s equal to 0.12 percent of the gross area for Slab A, and 0.23 percent for Slab B, did an excellent job of distributing cracks and keeping crack widths under control. In the case of Slab A, the amount of crack control steel was less than the 0.20 percent required by the ACI Code.

3. For load cases where cracks existed prior to loading, deflection computations based on gross cross-sectional properties may be too low, while computations based on the cracked section moment of inertia are too high. Deflection calculations based on an effective moment of inertia, similar to the method of Section 9.5.2 of ACI 318-77, give realistic though slightly conservative results as compared to those deflections measured in these tests.

4. There is a near-linear relationship between tendon stress increase and deflection, for a given initial tendon geometry.

5. Load capacity in all tests in which a failure occurred exceeded the factored load (1.4D + 1.7L) even though the tendons did not reach their ACI Code predicted stress.

6. For Slabs A and B, failure load ductility would have been increased and slightly higher ultimate load would have been observed with longer bottom bars in the exterior spans following ACI Code design requirements.

Acknowledgment

The experimental work reported in this study was performed at the Civil Engineering Structures Laboratory of The University of Texas at Austin, Austin, Texas. This work was sponsored by the Post-Tensioning Division of the Prestressed Concrete Institute (now the Post-Tensioning Institute) and their support is gratefully acknowledged.

References

1. ACI Committee 318, "Building Code Requirements for Reinforced Concrete (ACI 318-77)," American Concrete Institute, Detroit, Michigan, 1977.
2. Hemakom, R., "Behavior of Post-Tensioned Prestressed Concrete Slabs with Unbonded Reinforcement," Master's Thesis, The University of Texas at Austin, 1970.
3. Hemakom, R., "Behavior of Post-Tensioned Flat Plates with Unbonded Tendons," Doctor's Dissertation, The University of Texas at Austin, December, 1975.
4. Vines, W. R., "Strength and Behavior of a Post-Tensioned Slab with Unbonded Tendons," Master's Thesis, The University of Texas at Austin, May, 1976.
5. Charney, F. A., "Strength and Behavior of a Partially Prestressed Concrete Slab with Unbonded Tendons," Master's Thesis, The University of Texas at Austin, May, 1976.
6. Mattock, A. H., Yamazaki, J., and Kattula, B. T., "Comparative Study of Prestressed Concrete Beams With and Without Bond," *ACI Journal*, V. 68, No. 2, February, 1971, pp. 116-125.

* * *

Discussion of this report is invited. Please forward your comments to PCI Headquarters by March 1, 1979.